



Published in final edited form as:

*Clin Cancer Res.* 2017 February 15; 23(4): 1104–1116. doi:10.1158/1078-0432.CCR-16-1585.

## Neddylation E2 UBE2F promotes the survival of lung cancer cells by activating CRL5 to degrade NOXA via the K11 linkage

Weihua Zhou<sup>1</sup>, Jie Xu<sup>1</sup>, Haomin Li<sup>2,4</sup>, Ming Xu<sup>5</sup>, Zhijian J. Chen<sup>5,6</sup>, Wenyi Wei<sup>7</sup>, Zhenqiang Pan<sup>8</sup>, and Yi Sun<sup>1,2,3,\*</sup>

<sup>1</sup>Division of Radiation and Cancer Biology, Department of Radiation Oncology, University of Michigan, Ann Arbor, MI 48109, USA

<sup>2</sup>Institute of Translational Medicine, Zhejiang University School of Medicine, Hangzhou, Zhejiang, China

<sup>3</sup>Collaborative Innovation Center for Diagnosis and Treatment of Infectious Diseases, Zhejiang University, Hangzhou, P.R. China

<sup>4</sup>Children's Hospital, Zhejiang University School of Medicine, Hangzhou, Zhejiang, China

<sup>5</sup>Department of Molecular Biology, University of Texas Southwestern Medical Center, Dallas, TX 75390-9148, USA

<sup>6</sup>Howard Hughes Medical Institute, University of Texas Southwestern Medical Center, Dallas, TX 75390-9148, USA

<sup>7</sup>Department of Pathology, Beth Israel Deaconess Medical Center, Harvard Medical School, 3 Blackfan Circle, Boston, MA 02115, USA

<sup>8</sup>Departments of Oncological Sciences, Icahn School of Medicine at Mount Sinai, New York, NY 10029-6574, USA

### Abstract

**Purpose**—Recent studies have shown that the process of protein neddylation was abnormally activated in several human cancers. However, it is unknown whether and how UBE2F, a less characterized neddylation E2, regulates lung cancer cell survival, and whether and how NOXA, a pro-apoptotic protein, is ubiquitylated and degraded by which E3 and via which ubiquitin linkage.

**Experimental Design**—Methods of Immunohistochemistry and Immunoblotting were utilized to examine UBE2F protein expression. The biological functions of UBE2F were evaluated by *in vitro* cell culture and *in vivo* xenograft models. The *in vivo* complex formation among UBE2F-SAG-CUL5-NOXA was measured by pull-down assay. Poly-ubiquitylation of NOXA was evaluated by *in vivo* and *in vitro* ubiquitylation assays.

\*Corresponding author: Tel. 734-615-1989, Fax: 734-647-9654; sunyi@umich.edu.

**Author contributions:** W.Z., J.X., Z.C., W.W., Z.P., and Y.S. designed and directed the studies. W.Z., and J.X. performed experiments and analyzed the data. H.L. and M.X. performed data analysis. W.Z. and Y.S. wrote the paper.

**Conflict of interest:** All the authors declare no conflict of interest.

**Results**—UBE2F is overexpressed in NSCLC (Non-Small-Cell-Lung-Cancer), and predicts poor patient survival. While UBE2F overexpression promotes lung cancer growth both *in vitro* and *in vivo*, UBE2F knockdown selectively inhibits tumor growth. By promoting CUL5 neddylation, UBE2F/SAG/CUL5 tri-complex activates CRL5 (Cullin-RING-ligase-5) to ubiquitylate NOXA via a novel K11, but not K48, linkage for targeted proteasomal degradation. CRL5 inactivation or forced expression of K11R ubiquitin mutant caused NOXA accumulation to induce apoptosis, which is rescued by NOXA knockdown. Notably, NOXA knockdown rescues the UBE2F silencing effect, indicating a causal role of NOXA in this process. In lung cancer tissues, high levels of UBE2F and CUL5 correlate with low level of NOXA and poor patient survival.

**Conclusion**—By ubiquitylating and degrading NOXA through activating CRL5, UBE2F selectively promotes lung cancer cell survival and could, therefore, serve as a novel cancer target.

### Keywords

Cullin-RING ligase 5; Neddylation E2 enzyme; UBE2F; NOXA; Protein neddylation; K11 ubiquitylation linkage

### Introduction

Protein neddylation is a process of tagging NEDD8 (neural precursor cell expressed, developmentally downregulated 8), a ubiquitin-like molecule with 60% sequence identity to ubiquitin (1), to a lysyl residue of a substrate protein (2, 3) through a cascade catalyzed by three enzymes. The E1 NEDD8-activating enzyme (NAE), consisting of NAE1 (APP-BP1) and UBA3 (Ubiquitin Like Modifier Activating Enzyme 3) heterodimer; the E2 NEDD8-conjugating enzymes, and the E3 NEDD8 ligases, mainly consisting of a few RING domain-containing proteins, such as RBX1 (RING-box proteins 1) and RBX2, also known as SAG (Sensitive to Apoptosis Gene) [for review see (3)]. Involvement of the dysregulated neddylation modification in human lung cancer is supported by at least three pieces of evidence: 1) NEDD8 E3s DCUN1D1/SCCRO1/DCN1 (defective in cullin neddylation 1 domain containing 1/squamous cell carcinoma-related oncogene/defective in cullin neddylation) (4, 5) and DCUN1D5/SCCRO5/DCN5 (6) promote the proliferation and survival of squamous cell carcinomas of head & neck and lung; 2) NEDD8 E3 SAG is an anti-apoptotic protein with Kras-cooperative oncogenic activity in the lung (7); 3) over-expression and activation of the neddylation enzymes, including NEDD8, E1 (NAE1), and E2 (UBE2M (Ubiquitin Conjugating Enzyme E2 M)) were found in human lung cancer, whereas their inactivation suppressed tumor cell growth (8).

In mammalian cells, there are two neddylation E2s: well-studied UBE2M (also known as UBC12) and less characterized UBE2F (Ubiquitin Conjugating Enzyme E2 F). Both UBE2M and UBE2F bind to NEDD8 E1's ubiquitin-fold domain (ufd) and UBA3's hydrophobic groove via its core domains and N-terminal extension, respectively (9-12). Subsequent structural comparison however, revealed distinct features between UBE2F<sup>core</sup> and UBE2M<sup>core</sup> (12). Indeed, UBE2M and UBE2F are two independent E2s and show distinct functions. While UBE2M pairs with RBX1 to regulate neddylation of CUL1~4, UBE2F is largely specific for RBX2/SAG to mediate neddylation of CUL5 (12). Similar to UBE2M, which interacts with a hydrophobic pocket of DCN1 (Dcn1-like 1) PONY

domain via its N-acetyl-methionine (13), the N-terminally acetylated UBE2F also promotes cullin neddylation by binding to the PONY domains of DCNL2 and DCNL3 E3s, respectively (12, 14). Although UBE2M overexpression was found in lung cancer tissues (8), the involvement of UBE2F in lung cancer is completely unknown.

We have previously found that pro-apoptotic protein NOXA is subjected to negative regulation by SAG/RBX2 (15). However, it is unknown how SAG acts to shorten the protein half-life of NOXA. Also, it is controversial whether NOXA undergoes ubiquitylation-mediated degradation by proteasome (16-18). In the present study, we showed that UBE2F E2 couples with SAG E3 to induce CUL5 neddylation, leading to activation of CUL5 E3, which promotes NOXA poly-ubiquitylation via K11 linkage for proteasomal degradation. Thus, by promoting NOXA degradation, UBE2F exerts its growth-stimulating function. Finally, we found in lung cancer tissues, the high levels of UBE2F and CUL5 are correlated with the low level of NOXA, which is associated with poor survival of lung cancer patients. Taken together, we defined CUL5 as an E3 for NOXA via atypical K11 linkage and validated UBE2F as a potential lung cancer target and biomarker. Our study paves the road for future development of UBE2F inhibitors as a novel class of anticancer agents for selective cancer cell killing.

## Materials and methods

### Cloning of UBE2F-WT and -C116A mutant constructs

To clone wild type UBE2F, the human cDNA was PCR-amplified using the primers 5'-ATTGCGGCCGCTAACGCTAGCAAGTAACTGA-3' (5'-Not1) and 5'-CGCCTCGAGTCATCTGGCATAACGTTTGTAGTATCATC-3' (3'-Xho1), and then cloned into pCDNA3-HA<sub>3</sub> using Not1 and Xho1 sites. To clone UBE2F-C116A mutant, nested PCR was performed to obtain the DNA sequence containing the N-terminal fragment of UBE2F by using the primer 5'-Not1 and 5'-CTGTTAGCTGAAAAGCATGAAGCTTGTGTTGGA-3', and the C-terminal fragment of UBE2F by using primer 5'-CATGCTTTTCAGCTAACAGTAACCCAG-3' and 3'-Xho1. The two PCR products overlap with each other for 19 bp with introduced C116A mutation. The mixed N-terminal and C-terminal PCR fragments were used as a template to amplify the full-length UBE2F-C116A by using primer 5'-Not1 and 3'-Xho1, followed by cloning into pCDNA3-HA<sub>3</sub> using Not1 and Xho1 sites. All constructs were verified by DNA sequencing.

### The *in vivo* ubiquitylation assay

The 293 cells were co-transfected with various plasmids. The *in vivo* ubiquitylation assays were performed as previously described using Ni-beads pull-down (19).

### The *in vitro* ubiquitylation assay

FLAG-CUL5/-SAG or FLAG-CUL1/-RBX1 was transfected into 293 cells, respectively, and pulled down from the transfected cells by using FLAG beads, and used as the E3 complex. The reaction was carried out at 30 °C for 1 hr in 30 µl reaction buffer (40 mM Tris-HCl, pH 7.5, 2 mM DTT, 5 mM MgCl<sub>2</sub>) in the presence of purified NOXA protein (substrate), E1 (Boston Biochem), recombinant UBE2S/UBCH10 E2s (Boston Biochem), above E3

complexes, ATP, and ubiquitin (Boston Biochem). The reaction products were then resuspended in 25  $\mu$ l 2 $\times$ SDS-PAGE sample buffer for SDS-PAGE and detected by IB with antibody against NOXA (Rabbit; Santa Cruz).

### The *in vitro* neddylation assay

APP-BP1/UBA3 (7.5 nM), NEDD8 (2.5  $\mu$ M), UBE2F (3.4  $\mu$ M) or UBE2M (3.4  $\mu$ M), and co-purified full-length-SAG/truncated-CUL5 (398–780) proteins (0.25  $\mu$ M) were incubated in a reaction mixture (20  $\mu$ l), containing 50 mM Tris-HCl, pH7.4, 5 mM MgCl<sub>2</sub>, 2 mM ATP, 0.6 mM DTT, and 0.1 mg/ml BSA, with or without addition of MLN4924 for 10 min at room temperature, and then the reaction products were separated by 15% SDS-PAGE.

### NOXA half-life determination

For overexpression experiments, H358 cells were transiently transfected with indicated plasmids for 48 hrs, and then treated with 20  $\mu$ g/ml cycloheximide (CHX) for various periods of time, followed by IB. For silencing experiments, H358 cells were transfected with RNAi-1 against UBE2F, along with si-Cont, for 48 hrs, followed by CHX treatment and IB, using antibody against endogenous NOXA, with  $\beta$ -actin as the loading control. The relative NOXA levels were quantified by densitometry analysis using the ImageJ1.410 image processing software.

### *In vivo* antitumor study

All animal studies were conducted in accordance with the guidelines established by the University of Michigan Committee on Use and Care of Animals. To generate xenograft tumor models,  $5 \times 10^6$  H358 cells stably expressing pcDNA3 control, HA-UBE2F-WT, or HA-UBE2F-C116A were inoculated subcutaneously in both flanks of nude mice, followed by the measurement of tumor volume twice a week for up to 60 days.

### Statistical analysis

The Student's *t* test was used for the comparison of parameters between two groups. The correlation of the expression of two given proteins was assessed by Pearson correlation analysis. Survival was analyzed using the Kaplan-Meier method and compared by the log-rank test. Statistical Program for Social Sciences software 20.0 (SPSS, Chicago, IL) was used. All statistical tests were two-sided.

## Results

### UBE2F overexpression in human primary lung cancer tissues is associated with poor patient survival

Our recent study showed that the components of the neddylation process, including NEDD8, E1 (NAE1), E2 (UBC12/UBE2M), were highly expressed in lung cancer tissues, which is associated with poor overall survival of lung adenocarcinoma patients (8). To determine the potential involvement of UBE2F, a less characterized neddylation E2, in lung cancer, we performed immunohistochemistry (IHC) staining to measure the UBE2F level in a lung cancer tissue microarray, consisting of 128 adenocarcinomas (LUAD) and 40 squamous cell

carcinomas (LUSC), and scored results using receiver operating characteristic (ROC) curve analysis (20). As shown in Figure S1A, the UBE2F cutoff score for overall survival was 4.75 ( $p < 0.001$ ). We therefore divided the cohort into high (score  $\geq 4$ ) and low (score  $< 4$ ) expression based on the cutoff points (20) (Fig. 1A). More significantly, the Kaplan-Meier analysis showed that high UBE2F expression predicted a poor overall survival of lung cancer patients ( $n=168$ ;  $p=0.01$ ) (Fig. 1B) and for LUAD patients ( $n=128$ ;  $p=0.033$ ) (Fig. 1C), but not for LUSC patients ( $n=40$ ;  $p=0.266$ ) (Fig. 1D), which could be due to a limited number in the LUSC patient samples. Furthermore, Oncomine data analysis also revealed that compared to normal tissues, UBE2F mRNA was significantly elevated in LUAD in one study (21) (Fig. S1B), and in large cell lung carcinoma and LUAD but not LUSC, in another study (22) (Fig. S1C). These results therefore indicate that UBE2F is overexpressed in lung cancer tissues and may serve as a novel prognostic biomarker for LUAD patients.

### **UBE2F overexpression promotes growth of lung cancer cells *in vitro* and *in vivo***

We next determined the biological significance of elevated UBE2F expression in lung cancer cells. We found that ectopic expression of wild type (WT) UBE2F at a level comparable to endogenous level (Figs. 1E and S1D) promoted cell survival as measured by ATP-lite and colony formation assays, whereas similar expression of a catalytically inactive UBE2F mutant (C116A), suppressed the growth and survival of lung cancer cells (Figs. 1F&G; Figs. S1E&F). Thus, UBE2F appears to have growth-promoting activity with its enzymatic dead mutant acting likely in a dominant negative manner.

We next determined growth promoting activity of UBE2F using an *in vivo* xenograft tumor model and found when compared to the vector control, UBE2F-WT promoted *in vivo* tumor growth, whereas UBE2F-C116A mutant suppressed it ( $p < 0.05$ , Fig. 1H). Consistently, the average tumor size/weight at the end of the experiment (day 60) was the highest in the UBE2F-WT group and lowest in the UBE2F-C116A mutant group, which are statistically different from the vector control and between each other (Fig. 1I). We further confirmed that both UBE2F-WT and -C116A mutant were indeed expressed in tumor tissues (Fig. S1G), and our IHC staining of tumor tissues revealed that compared to the vector control, UBE2F-WT promoted survival (Ki-67) and inhibited apoptosis (cleavage caspase-3 and NOXA), whereas UBE2F-C116A mutant had an opposite effect (Figs. 1J&K). Collectively, the results from both *in vitro* cell culture and *in vivo* xenograft models coherently demonstrated that UBE2F-WT promoted cell growth and survival, whereas the C116A enzymatically dead mutant acted in a dominant negative manner to suppress growth and survival of lung cancer cells.

### **UBE2F silencing inhibits cell growth by inducing apoptosis**

We further validated UBE2F as an appealing cancer drug target using the siRNA-mediated silencing approach in two lung cancer cell lines, along with immortalized bronchial epithelial Beas-2B cells, serving as a “normal” control. Interestingly, UBE2F depletion caused suppression of cell survival, as measured by ATP-lite assay in both H358 and A427 cells, whereas it had no effect on Beas-2B normal cells (Fig. 2A), demonstrating a tumor cell specific effect consistent with a previous study that UBE2F knockdown inhibited the growth of HeLa cells, but not immortalized NIH3T3 cells (12). Furthermore, clonogenic survival of

both cancer cell lines was also significantly suppressed upon UBE2F silencing ( $p < 0.01$ ; Figs. 2B&C). The nature of suppression in survival upon UBE2F depletion was via induction of apoptosis in both H358 and A427 cells, but not in Beas-2B cells, as evidenced by cleavage of PARP and caspase-3 (Fig. 2D), as well as the induction of DNA fragmentation (Fig. 2E). Thus, growth suppression upon UBE2F depletion is mediated via apoptosis induction. Taken together, both gain-of-function and loss-of-function experiments strongly suggested that UBE2F could be a novel therapeutic target for lung cancer.

We finally applied a pharmaceutical approach to validate neddylation modification, including UBE2F, as an attractive lung cancer target by using an *in vivo* xenograft model. Treatment of H358 xenograft tumor-bearing mice with MLN4924, a small molecule inhibitor of NAE (23), to block the entire process of neddylation modification, significantly suppressed tumor growth (Fig. S2A&B). The effect on normal tissues was minimal, if at all, as reflected by relatively unchanged body weight during drug treatment (Fig. S2C). Importantly, MLN4924 indeed hit the target as demonstrated by cullin-1 deneddylation in tumor tissues (Fig. S2D), and suppressed survival and induced apoptosis (Figs. S2E&F).

### UBE2F negatively regulates pro-apoptotic NOXA levels in lung cancer cells

We have previously shown that SAG/RBX2 negatively regulates NOXA with an unknown mechanism (15). Given SAG couples with UBE2F to neddylate CUL5 (12), we first systematically measured NOXA levels upon siRNA-based silencing of three components of CRL5, including UBE2F, SAG and CUL5, individually. As a comparison, we also silenced three components of CRL1 including UBE2M, RBX1, and CUL1. In both H358 (Fig. 3A) and A427 (Fig. S3A) lung cancer cells, depletion of UBE2F, SAG or CUL5 decreased CUL5 neddylation and caused significant accumulation of NOXA, whereas depletion of UBE2M, RBX1, or CUL1, reduced CUL1 neddylation, but failed to increase NOXA level. The results clearly showed that NOXA levels are subjected to regulation by CRL5 but not by CRL1. It is worth noting that silencing SAG decreased UBE2F, and vice versa (data not shown). Given that UBE2F and SAG are neddylation E2 and E3 for CUL5 neddylation, respectively, it is very likely that they form the complex *in vivo*, which is much more stable than their respective free form.

We then focused our study on UBE2F and determined its role in modulating CRL5. Using both gain-of-function and loss-of-function approaches we found that in both lung cancer cell lines, overexpression of UBE2F-WT, but not its enzymatically dead mutant UBE2F-C116A, increased CUL5 neddylation (Figs. 3B&S3B). Moreover, UBE2F depletion largely eliminated CUL5 neddylation (Figs. 3C&S3C) without much effect on Beas-2B normal cells (Fig. S3D), indicating that UBE2F effect is highly cullin-5 and cancer cell specific at the cellular levels. Neither approach had any significant effect on the neddylation of all other cullins, including cullin-1, -2, -3, -4A and -4B in both lung cancer cell lines (Figs. 3B&C and S3B&C).

Given that UBE2F is specific for neddylation of CUL5 leading to CRL5 activation (12) to promote the ubiquitylation and degradation of substrates, we measured the levels of a few reported CRL5 substrates, including the host antiviral factor APOBEC3G (apolipoprotein B mRNA editing enzyme, catalytic polypeptide-like 3G (A3G)) (24), active phospho-Src (25),



and Dab1 (Disable-1) (26), along with a few CRL1 substrates known to regulate proliferation (p21, p27) and apoptosis (Bim). Ectopic expression of neither UBE2F-WT nor -C116A mutant caused any significant accumulation of these reported substrates for CRL5 or CRL1 except NOXA, which was decreased or increased upon overexpression of UBE2F-WT or C116A, respectively (Fig. 3D). Likewise, depletion of UBE2F had no effect on the levels of these reported substrates of CRL5 and CRL1 except NOXA, which was accumulated (Figs. 3E&S3E). Interestingly, UBE2F deletion did not cause NOXA accumulation in normal Beas-2B cells (Fig. S3D), further suggesting that UBE2F effect is cancer cell specific. Taken together, UBE2F negatively regulates NOXA protein levels.

We next determined whether UBE2F regulates NOXA protein half-life. Compared with the vector control, UBE2F-WT overexpression decreased the basal level of endogenous NOXA and shortened its protein half-life from ~1 hr to 30 min, whereas UBE2F-C116A overexpression increased the basal level of endogenous NOXA and extended NOXA protein half-life to ~1.5 hrs (Figs. 3F&G). Notably, effect of UBE2F on NOXA can be completely reversed by the proteasome inhibitor MG132 (Fig. S3F), indicating that UBE2F-mediated NOXA degradation is proteasome-dependent. Consistently, UBE2F depletion by siRNA silencing significantly extended protein half-life of endogenous NOXA up to 2 hrs (Figs. 3H&I). Taken together, our results demonstrate that UBE2F reduces the NOXA levels by shortening its protein half-life.

#### UBE2F-activated CRL5 promotes NOXA poly-ubiquitylation via the K11 linkage

We further investigated whether NOXA is indeed a *bona fide* substrate of CRL5, but not CRL1. We first found that ectopically expressed CUL5 pulled down endogenous SAG, UBE2F, and NOXA, showing that neddylation E2/E3 formed a complex with its substrate *in vivo*, whereas ectopically expressed CUL1 only showed a strong binding with endogenous RBX1, and UBE2M, with a weak binding to SAG (Fig. 4A), indicating that NOXA is physically bound to CRL5, but not CRL1.

UBE2F has been previously reported to co-operate with SAG/RBX2 E3 to promote CUL5 neddylation (12). To confirm this, we performed an *in vitro* neddylation assay by using purified neddylation E1, E2 (UBE2F or UBE2M), E3 (co-purified full-length-SAG/truncated-CUL5 (398–780) proteins), and NEDD8 in a reaction mixture with or without addition of MLN4924, a small molecule inhibitor of NAE (23). Our results showed that UBE2F, but not UBE2M, promoted CUL5 neddylation, which could be blocked by MLN4924 (Fig. 4B), demonstrating that UBE2F can indeed activate CRL5 by promoting CUL5 neddylation in our system.

It is currently controversial whether NOXA degradation by proteasome is mediated via ubiquitylation. Two previous studies suggested it is ubiquitylation independent (16, 17), whereas the third study showed that it is dependent via the K48 linkage (18). We, therefore, determined whether NOXA is subjected to poly-ubiquitylation by CRL5 and if so, by which lysine/K linkage. We first performed a cell-based (*in vivo*) ubiquitylation assay by using wild-type ubiquitin (WT-Ub), ubiquitin mutants with specific K replaced by R (arginine) (KR-Ub), or an ubiquitin mutant with all K replaced by R (K0-Ub). The results showed that when wt ubiquitin was used, NOXA can be poly-ubiquitylated by an E3 complex purified

from cell lysates after co-transfection of UBE2F-SAG-CUL5 (Fig. 4C). Interestingly, NOXA poly-ubiquitylation can also be seen when K48R or K63R mutants, but not K0 or K11R was used as the ubiquitin source (Fig. 4C), strongly suggesting that NOXA poly-ubiquitylation is via the K11 linkage. We further confirmed the finding by utilizing a series of ubiquitin mutants, containing only one indicated lysine, while all six other lysine residues replaced by arginine residues (K-Ub) in the same assay. Compared to WT-Ub, K11-Ub was the only ubiquitin mutant that retained NOXA poly-ubiquitylation (Fig. 4D).

To further demonstrate that NOXA is a *bona fide* substrate of CRL5 but not CRL1, we compared the poly-ubiquitylation of NOXA and p27 by co-transfection of UBE2M/RBX1/CUL1 (CRL1 complex), or UBE2F/SAG/CUL5 (CRL5 complex) respectively. While the CRL1 specifically promoted the p27 poly-ubiquitylation, CRL5 promoted only NOXA poly-ubiquitylation (Figs. S4A&B). To further identify the ubiquitylation site(s) on NOXA catalyzed by CRL5, we transfected 293 cells with His-tagged NOXA and its various K mutants (17), in which the K residues of the wild-type NOXA were changed to R residues in various combinations, and performed the *in vivo* ubiquitylation assay. The results showed that NOXA C3KR mutants with three C-terminal K residues K35, K41, and K48 simultaneously replaced by three R residues, had a complete elimination of ubiquitylation, whereas the ubiquitylation of any other mutants remained (Fig. S4C).

Two previous studies reported that NOXA is degraded in an ubiquitin-independent manner (16, 17). However, both studies failed to compare NOXA protein half-life using wt vs. various NOXA mutants in the same Western Blotting. To ensure a fair comparison, we measure protein half-life of wt vs. C3KR mutant by including them in the same Western Blotting. Our results convincingly showed that the half-life of exogenously expressed His-tagged NOXA-WT is significantly shorter than that of NOXA-C3KR (Fig. S4D; compare lanes 6-10 vs. 11-15). Furthermore, co-transfection of UBE2F-WT significantly shortened the half-life of exogenous NOXA-WT but not C3KR mutant (Fig. S4E; compare lanes 5-8 and 9-12). Collectively, our data showed that NOXA is a *bona fide* substrate of UBE2F/CRL5 with ubiquitylation occurring at anyone or all three carboxyl-terminal lysine residues (K35/41/48).

To further confirm the finding, we performed an *in vitro* ubiquitylation assay by using K11-specific E2s. It was previously shown that K11 specificity is determined by an E2 enzyme, UBE2S, which elongates ubiquitin chains after the substrates are pre-ubiquitylated by UBCH10 (27, 28). To do this, we pulled down FLAG-CUL5/-SAG or FLAG-CUL1/-RBX1 (E3s) using bead-conjugated FLAG antibody from transfected 293 cells, and then added it, as E3 source, into an *in vitro* ubiquitylation reaction mixture, containing purified NOXA protein (substrate), E1, E2s (UBE2S and UBCH10), purified wild-type ubiquitin (WT-Ub) and a series of ubiquitin mutants with K-to-R replacement (KR-Ub). We found that in the reaction mixture with K11-specific E2s, all forms of ubiquitin, except the K11R mutant, showed long poly-ubiquitylation chains (Fig. 4E, lane 5-8). Consistently, no NOXA poly-ubiquitylation was seen when CUL1-RBX1 was used as E3 source (Fig. 4E, lane 9). We further confirmed the finding by using K11, K48, and K63 mutants (only indicated lysine residue in wt form). Indeed, in addition to wt ubiquitin, only K11 mutant showed NOXA ubiquitylation chain (Figure 4F). Taken together, our data clearly demonstrated that CRL5,



activated by UBE2F/SAG, but not CRL1, promotes NOXA poly-ubiquitylation for subsequent proteasomal degradation, via not conventional K48 linkage but the K11 linkage, which is also implicated for proteasomal degradation (29).

### **NOXA is selectively accumulated in U2OS-shUb-Ub (K11R) cells and responsible for apoptotic phenotype**

To further demonstrate that NOXA is degraded via K11 linkage but not the conventional K48 linkage at the cellular level, we detected NOXA expression in U2OS cells where endogenous ubiquitin was deleted and replaced with K11R, K48R and K63R mutants, respectively, using a tetracycline-inducible system (30). To characterize the efficiency of ubiquitin knockdown and replacement upon tetracycline treatment in these cell lines, we carried out RT-PCR (reverse transcription-polymerase chain reaction) analyses using primers that distinguish endogenous and exogenous ubiquitin genes (30). The results showed that the expression of all four endogenous ubiquitin genes UBA52 (Ubiquitin A-52 Residue Ribosomal Protein Fusion Product 1), UBB (ubiquitin B), UBC (ubiquitin C), and RPS27A (Ribosomal Protein S27a), was reduced by 80%–95%, and the expression of the ubiquitin transgenes, UB', was dramatically induced when the cells were grown in the presence of tetracycline for 4 days (Fig. S5A). NOXA was then found to be accumulated at the highest level in tetracycline-inducible K11R cells (Fig. 5A, lane 4) with p21, p27, and Bim, which are all degraded through the K48 linkage, accumulated most obviously in tetracycline-inducible K48R cells (Fig. 5A, lane 6), further demonstrating that the K11 linkage but not K48 linkage is involved in the proteasomal degradation of NOXA. Moreover, we found that tetracycline treatment inhibited cell growth and induced apoptosis most significantly seen in K11R cells (Fig. S5B) as evidenced by increased cleavage of PARP and caspase-3 (Fig. 5B), as well as increased DNA fragmentation (Fig. 5C). Simultaneous NOXA knockdown could largely reverse growth inhibition (Fig. 5D) and apoptotic phenotypes (Figs. 5E&F) caused by tetracycline treatment, which triggered the expression of degradation-resistant NOXA in the K11R cells. Thus, it appears that NOXA plays a causal role in apoptosis induction under these experimental conditions.

### **NOXA depletion partially rescues phenotype triggered by UBE2F knockdown**

We finally determined whether NOXA accumulation played a causal role in apoptosis induction triggered by UBE2F depletion in H358 cells via a functional rescuing experiment. Indeed, growth suppression and apoptosis triggered by UBE2F depletion were largely abrogated by simultaneous depletion of NOXA, as measured by ATP-lite assay ( $p < 0.01$ ; Fig. 5G), clonogenic survival assay ( $p < 0.01$ ; Fig. 5H), and IB for apoptotic cleavage of PARP and caspase-3 (Fig. 5I). Thus, NOXA ubiquitylation and subsequent degradation plays a causal role in UBE2F-induced growth promotion of lung cancer cells.

### **Expression of UBE2F, CUL5 and NOXA in human primary lung cancer tissues and their association with patient survival**

Finally, we compared whether expression of UBE2F, CUL5 and NOXA is correlated in lung cancer tissues and whether their expression is associated with patient survival. We performed IHC staining for CUL5 and NOXA in a lung cancer tissue microarray and scored results by analysis of ROC curve, as we did for UBE2F IHC staining (Fig. 1A&S1A). As

shown in Figure S6A, ROC analysis revealed that the score of 4.25 and 2.25 were the cutoff points for CUL5 and NOXA, respectively, to distinguish the tumor samples as being high or low expressers (Fig. S6A&B).

Based upon ROC cutoff points, the levels of UBE2F and CUL5 expression were inversely correlated with the level of NOXA expression in the same sets of samples (Fig. 6A). Specifically, in a total of 168 NSCLC cases studied, UBE2F was highly expressed in 97 (97/168; 57.7%) tumor tissues, of which 73 (73/97; 75.3%) showed an elevated CUL5 expression and 74 (74/97; 76.3%) showed a decreased NOXA expression (Fig. S6C). The correlation coefficient ( $r^2$ ) for UBE2F and CUL5 is 0.651, and for UBE2F and NOXA is -0.339, which are both statistically significant ( $p < 0.001$ ) (Fig. S6C). More significantly, we analyzed the correlation among co-overexpression of UBE2F and CUL5 vs. NOXA with patient survival and found that in 97 NSCLC patients with elevated UBE2F expression, the subset with higher CUL5 ( $n=73$ ) showed a worse overall survival, as compared with those with low CUL5 expression ( $p=0.001$ ; Fig. 6B). On the other hand, patients with low NOXA expression ( $n=74$ ) within the high UBE2F expression group ( $n=97$ ) showed poorer overall survival compared with those with high NOXA expression ( $p=0.005$ ; Fig. 6C). Thus, high frequency of co-overexpression of UBE2F and CUL5 coupled with low expression of NOXA in lung cancer suggests that CUL5 activation via neddylation (by UBE2F) to promote NOXA degradation may actually occur during human lung tumorigenesis.

## Discussion

Accumulated data suggest that altered protein neddylation is actively involved in the tumorigenesis, as evidenced by a growing list of NEDD8 substrates with oncogenic implications (2) and the pro-survival roles of a variety of neddylation E3s in cancers (4-7). Our recent study further demonstrates that the components of protein neddylation process, including NEDD8, E1 (NAE1), E2 (UBE2M) are over-expressed in lung cancer tissues, whereas knockdown of these components suppresses the growth of cancer cells (8). However, how UBE2F, a less characterized NEDD8 E2, acts in lung cancer is largely unknown. In the present study, we report a growth promoting function of UBE2F, as supported by the following pieces of evidence: 1) UBE2F is over-expressed in NSCLC tissues and its overexpression is associated with poor prognosis of patients with lung adenocarcinomas (Fig. 1A-D); 2) overexpression of UBE2F-WT promotes, whereas overexpression of catalytic inactive UBE2F mutant (C116A) inhibits the growth of lung cancer cells both *in vitro* culture and *in vivo* xenograft models (Fig. 1E-K); and 3) UBE2F knockdown significantly inhibits the growth of lung cancer cells by inducing apoptosis (Fig. 2).

Cullin neddylation has been shown to increase the ligase activity of CRLs, thus promoting the ubiquitylation and degradation of their protein substrates. In this study, we identified that pro-apoptotic protein NOXA is a *bona fide* substrate of CRL5, but not CRL1, E3 ligase for targeted ubiquitylation and degradation with the following pieces of supporting evidence: 1) NOXA level decreases upon UBE2F-WT overexpression, but increases upon UBE2F-C116A overexpression or UBE2F depletion; 2) NOXA protein half-life is shortened upon UBE2F overexpression and extended upon UBE2F depletion; 3) NOXA forms a complex

with the UBE2F/SAG/CUL5; 4) CRL5, but not CRL1, promotes poly-ubiquitylation of NOXA at the C-terminal three lysine residues, as measured by both *in vivo* and *in vitro* ubiquitylation assays.

The ubiquitin-proteasome system (UPS) fulfills essential cellular functions in eukaryote organisms through timely degradation of a variety of regulatory proteins (31). It is established that NOXA is a short-lived protein and subjected to ubiquitylation (32). However, it is controversial whether proteasome-mediated degradation of NOXA is ubiquitylation dependent or independent. Two studies suggested that it is ubiquitylation-independent since a ubiquitylation-resistant K-to-R mutant of NOXA has a similar protein half-life as the wt NOXA (16, 17), whereas a third study showed that NOXA is subjected to K48-linked ubiquitylation and its removal by deubiquitylating enzyme UCH-L1 (Ubiquitin C-Terminal Hydrolase L1) protects NOXA from proteasome degradation (18). Nevertheless, all three studies did not identify any E3s responsible for NOXA poly-ubiquitylation. Furthermore, the first two studies did not compare NOXA protein half-life using wt vs. various NOXA mutants run in the same Western blot. Here, we demonstrated that exogenously expressed NOXA-WT clearly shows a much shorter half-life, compared to a C-terminal lysine-free mutant (C3KR) in the same Western blot (Fig. S4D). Furthermore, co-transfected UBE2F significantly shortened the half-life of exogenous NOXA-WT, but had little, if any, effect on the half-life of exogenous NOXA-C3KR (Fig. S4E). Accordingly, in our system, we identified and characterized that CRL5 is a *bona fide* E3 that mediates the ubiquitylation and subsequent degradation of NOXA.

Polyubiquitin chains are assembled via one of seven lysine residues or the N terminus. While the essential roles of K48-linked chains in proteasomal degradation (33) and K63-linked chains in cell signaling (34) have been well characterized, the functions of the remaining 'atypical' ubiquitin chain types are less well defined. Recent work has implicated that K11-linked polyubiquitin chains serve as a degradation signal for APC/C substrates in regulation of cell division (35, 36). The APC/C can utilize 'priming' E2 enzymes such as UBE2C (also known as UBCH10) or UBE2D (also called UBCH5 or UBC4) (36, 37) to decorate substrates with mono-ubiquitin and short ubiquitin chains, which were subsequently extended by the K11-specific 'elongating' E2 enzyme (UBE2S) into long K11-linked ubiquitin polymers (27, 28). Long K11-linked polyubiquitin chains are assembled by the APC/C (Anaphase-Promoting Complex/cyclosome) in a single substrate binding event, and then promote rapid degradation of modified proteins during cell cycle progression (27, 36, 38). K11 linkages were also identified in the context of mixed ubiquitin chains in several cellular processes, including endoplasmic reticulum associated degradation (ERAD) (39), membrane trafficking (40) and TNF $\alpha$  (tumor necrosis factor  $\alpha$ ) signaling (41). Many described cellular pathways that function by utilizing K11 linkages are involved in human disease, and overexpression of the K11-specific E2 enzymes UBE2C and UBE2S has been associated with cancer [for review, see (29)]. Here, we clearly showed using various ubiquitin mutants in both *in vivo* and *in vitro* ubiquitylation assays that the linkage of NOXA poly-ubiquitylation mediated by UBE2F-activated CRL5 E3 is not through conventional K48, rather through atypical K11. To the best of our knowledge, this is the first study reporting that in addition to APC/C E3, CRL5 can also promote K11-linked poly-ubiquitylation. It is worth noting that until now poly-ubiquitylation of all substrates known

to be induced by CRL E3 for proteasomal degradation is mediated via the K48-linked ubiquitin chain.

We used ubiquitin replacement strategy (30) to investigate the function of polyubiquitin topology in degradation of CRL substrates and regulation of apoptosis. We found that among 4 CRL substrates tested, using wt and three ubiquitin mutants, the K11 linked ubiquitylation regulates NOXA (novel finding of this study), whereas the K48 linked ubiquitylation regulates p21, p27, and Bim (which is well-established). Furthermore, expression of K11R caused the most substantial growth suppression due to induction of apoptosis, which is mainly attributable to accumulated NOXA due to lack of degradation, since depletion of NOXA can largely reverse apoptotic phenotype. Thus, CRL5-induced NOXA ubiquitylation via the K11-linkage for targeted degradation plays an essential role in apoptosis regulation.

Deregulation of various components of the ubiquitin-proteasome system (UPS) (42), which maintains the protein homeostasis by timely degradation of unwanted proteins, has been observed in lung cancer (43, 44). We have previously shown that SAG, a neddylation and ubiquitylation E3, is overexpressed in lung cancer with poor patient survival (7, 15). Here we showed that neddylation E2 UBE2F is also overexpressed in lung cancer. More importantly, co-overexpression of UBE2F-CUL5, coupled with down regulation of NOXA is significantly correlated with poor survival of lung cancer patients. This association study suggests that activation of CRL5 with consequent degradation of NOXA could be a frequent event during lung tumorigenesis.

In summary, our study supports the following model. While UBE2M couples with RBX1 to neddylate CUL1-4, thus activating CRL1-4 for targeted degradation of their substrates (such as p21, p27, Bim) via K48-linked ubiquitylation, UBE2F couples with SAG/RBX2 to neddylate CUL5 for CRL5 activation and subsequent ubiquitylation and degradation of NOXA via the K11-linkage. Overexpression of UBE2F (E2) and CUL5 (this study), and SAG (E3) (15) in lung cancer cells would promote NOXA degradation, leading to blockage of apoptosis for increased cell survival. Thus, targeting the UBE2F/SAG/CRL5 axis either by small molecule inhibitor such as MLN4924, or by genetic depletion of either component would inactivate CRL5 to cause NOXA accumulation and apoptosis induction, thus antagonizing UBE2F-mediated growth-stimulating processes (Fig. 6D). Overall, our study provides convincing experimental evidence to show that the UBE2F/SAG/CRL5 axis is a valid and attractive drug target. Given the fact that depletion of UBE2F, but not UBE2M (12) selectively suppresses growth of lung cancer cells, but not normal cells (Fig. 2B), targeting UBE2F, rather than UBE2M, could be a preferred approach for anti-cancer therapy.

## Supplementary Material

Refer to Web version on PubMed Central for supplementary material.

## Acknowledgments

We would like to thank Dr. Wei Gu for providing us ubiquitin mutants, Dr. Dongping Wei for the cloning of wild-type and mutant UBE2F constructs, and Dr. Xu Luo for providing us His-NOXA and its lysine mutants.

**Financial support:** This work is supported by the NCI grants CA118762, CA156744, and CA171277 (YS), by Chinese Minister of Science and Technology grant 2016YFA0501800 (YS), and by the Chinese NSFC Grants 81572718 (YS) and 31528015 (WW). The author (YS) also gratefully acknowledges the support of K. C. Wong Education Fund.

## References

1. Kamitani T, Kito K, Nguyen HP, Yeh ET. Characterization of NEDD8, a developmentally down-regulated ubiquitin-like protein. *The Journal of biological chemistry*. 1997; 272:28557–62. [PubMed: 9353319]
2. Watson IR, Irwin MS, Ohh M. NEDD8 pathways in cancer, *Sine Quibus Non*. *Cancer cell*. 2011; 19:168–76. [PubMed: 21316600]
3. Zhao Y, Morgan MA, Sun Y. Targeting Neddylolation Pathways to Inactivate Cullin-RING Ligases for Anticancer Therapy. *Antioxidants & redox signaling*. 2014; 21:2383–400. [PubMed: 24410571]
4. Sarkaria I, Oc P, Talbot SG, Reddy PG, Ngai I, Maghami E, et al. Squamous cell carcinoma related oncogene/DCUN1D1 is highly conserved and activated by amplification in squamous cell carcinomas. *Cancer research*. 2006; 66:9437–44. [PubMed: 17018598]
5. Singh B, Stoffel A, Gogineni S, Poluri A, Pfister DG, Shaha AR, et al. Amplification of the 3q26.3 locus is associated with progression to invasive cancer and is a negative prognostic factor in head and neck squamous cell carcinomas. *The American journal of pathology*. 2002; 161:365–71. [PubMed: 12163360]
6. Bommelje CC, Weeda VB, Huang G, Shah K, Bains S, Buss E, et al. Oncogenic function of SCCRO5/DCUN1D5 requires its Neddylolation E3 activity and nuclear localization. *Clinical cancer research : an official journal of the American Association for Cancer Research*. 2014; 20:372–81. [PubMed: 24192928]
7. Li H, Tan M, Jia L, Wei D, Zhao Y, Chen G, et al. Inactivation of SAG/RBX2 E3 ubiquitin ligase suppresses KrasG12D-driven lung tumorigenesis. *J Clin Invest*. 2014; 124:835–46. [PubMed: 24430184]
8. Li L, Wang M, Yu G, Chen P, Li H, Wei D, et al. Overactivated neddylation pathway as a therapeutic target in lung cancer. *Journal of the National Cancer Institute*. 2014; 106:dju083. [PubMed: 24853380]
9. Huang DT, Hunt HW, Zhuang M, Ohi MD, Holton JM, Schulman BA. Basis for a ubiquitin-like protein thioester switch toggling E1-E2 affinity. *Nature*. 2007; 445:394–8. [PubMed: 17220875]
10. Huang DT, Miller DW, Mathew R, Cassell R, Holton JM, Roussel MF, et al. A unique E1-E2 interaction required for optimal conjugation of the ubiquitin-like protein NEDD8. *Nature structural & molecular biology*. 2004; 11:927–35.
11. Huang DT, Paydar A, Zhuang M, Waddell MB, Holton JM, Schulman BA. Structural basis for recruitment of Ubc12 by an E2 binding domain in NEDD8's E1. *Molecular cell*. 2005; 17:341–50. [PubMed: 15694336]
12. Huang DT, Ayrault O, Hunt HW, Taherbhoy AM, Duda DM, Scott DC, et al. E2-RING expansion of the NEDD8 cascade confers specificity to cullin modification. *Molecular cell*. 2009; 33:483–95. [PubMed: 19250909]
13. Scott DC, Monda JK, Bennett EJ, Harper JW, Schulman BA. N-terminal acetylation acts as an avidity enhancer within an interconnected multiprotein complex. *Science*. 2011; 334:674–8. [PubMed: 21940857]
14. Monda JK, Scott DC, Miller DJ, Lydeard J, King D, Harper JW, et al. Structural conservation of distinctive N-terminal acetylation-dependent interactions across a family of mammalian NEDD8 ligation enzymes. *Structure*. 2013; 21:42–53. [PubMed: 23201271]
15. Jia L, Yang J, Hao X, Zheng M, He H, Xiong X, et al. Validation of SAG/RBX2/ROC2 E3 ubiquitin ligase as an anticancer and radiosensitizing target. *Clinical cancer research : an official journal of the American Association for Cancer Research*. 2010; 16:814–24. [PubMed: 20103673]
16. Craxton A, Butterworth M, Harper N, Fairall L, Schwabe J, Ciechanover A, et al. NOXA, a sensor of proteasome integrity, is degraded by 26S proteasomes by an ubiquitin-independent pathway that is blocked by MCL-1. *Cell death and differentiation*. 2012; 19:1424–34. [PubMed: 22361683]



17. Pang X, Zhang J, Lopez H, Wang Y, Li W, O'Neill KL, et al. The carboxyl-terminal tail of Noxa protein regulates the stability of Noxa and Mcl-1. *The Journal of biological chemistry*. 2014; 289:17802–11. [PubMed: 24811167]
18. Brinkmann K, Zigrino P, Witt A, Schell M, Ackermann L, Broxtermann P, et al. Ubiquitin C-terminal hydrolase-L1 potentiates cancer chemosensitivity by stabilizing NOXA. *Cell reports*. 2013; 3:881–91. [PubMed: 23499448]
19. Zhou W, Xu J, Zhao Y, Sun Y. SAG/RBX2 is a novel substrate of NEDD4-1 E3 ubiquitin ligase and mediates NEDD4-1 induced chemosensitization. *Oncotarget*. 2014; 5:6746–55. [PubMed: 25216516]
20. Zhou WH, Tang F, Xu J, Wu X, Yang SB, Feng ZY, et al. Low expression of Beclin 1, associated with high Bcl-xL, predicts a malignant phenotype and poor prognosis of gastric cancer. *Autophagy*. 2012; 8:389–400. [PubMed: 22240664]
21. Okayama H, Kohno T, Ishii Y, Shimada Y, Shiraishi K, Iwakawa R, et al. Identification of genes upregulated in ALK-positive and EGFR/KRAS/ALK-negative lung adenocarcinomas. *Cancer research*. 2012; 72:100–11. [PubMed: 22080568]
22. Hou J, Aerts J, den Hamer B, van Ijcken W, den Bakker M, Riegman P, et al. Gene expression-based classification of non-small cell lung carcinomas and survival prediction. *PloS one*. 2010; 5:e10312. [PubMed: 20421987]
23. Soucy TA, Smith PG, Milhollen MA, Berger AJ, Gavin JM, Adhikari S, et al. An inhibitor of NEDD8-activating enzyme as a new approach to treat cancer. *Nature*. 2009; 458:732–6. [PubMed: 19360080]
24. Yu X, Yu Y, Liu B, Luo K, Kong W, Mao P, et al. Induction of APOBEC3G ubiquitination and degradation by an HIV-1 Vif-Cul5-SCF complex. *Science*. 2003; 302:1056–60. [PubMed: 14564014]
25. Laszlo GS, Cooper JA. Restriction of Src activity by Cullin-5. *Current biology : CB*. 2009; 19:157–62. [PubMed: 19147357]
26. Feng L, Allen NS, Simo S, Cooper JA. Cullin 5 regulates Dab1 protein levels and neuron positioning during cortical development. *Genes & development*. 2007; 21:2717–30. [PubMed: 17974915]
27. Wu T, Merbl Y, Huo Y, Gallop JL, Tzur A, Kirschner MW. UBE2S drives elongation of K11-linked ubiquitin chains by the anaphase-promoting complex. *Proceedings of the National Academy of Sciences of the United States of America*. 2010; 107:1355–60. [PubMed: 20080579]
28. Williamson A, Wickliffe KE, Mellone BG, Song L, Karpen GH, Rape M. Identification of a physiological E2 module for the human anaphase-promoting complex. *Proceedings of the National Academy of Sciences of the United States of America*. 2009; 106:18213–8. [PubMed: 19822757]
29. Bremm A, Komander D. Emerging roles for Lys11-linked polyubiquitin in cellular regulation. *Trends in biochemical sciences*. 2011; 36:355–63. [PubMed: 21641804]
30. Xu M, Skaug B, Zeng W, Chen ZJ. A ubiquitin replacement strategy in human cells reveals distinct mechanisms of IKK activation by TNFalpha and IL-1beta. *Molecular cell*. 2009; 36:302–14. [PubMed: 19854138]
31. Vucic D, Dixit VM, Wertz IE. Ubiquitylation in apoptosis: a post-translational modification at the edge of life and death. *Nature reviews Molecular cell biology*. 2011; 12:439–52. [PubMed: 21697901]
32. Baou M, Kohlhaas SL, Butterworth M, Vogler M, Dinsdale D, Walewska R, et al. Role of NOXA and its ubiquitination in proteasome inhibitor-induced apoptosis in chronic lymphocytic leukemia cells. *Haematologica*. 2010; 95:1510–8. [PubMed: 20378569]
33. Komander D, Rape M. The ubiquitin code. *Annual review of biochemistry*. 2012; 81:203–29.
34. Chen ZJ, Sun LJ. Nonproteolytic functions of ubiquitin in cell signaling. *Mol Cell*. 2009; 33:275–86. [PubMed: 19217402]
35. Kirkpatrick DS, Hathaway NA, Hanna J, Elsasser S, Rush J, Finley D, et al. Quantitative analysis of in vitro ubiquitinated cyclin B1 reveals complex chain topology. *Nature cell biology*. 2006; 8:700–10. [PubMed: 16799550]
36. Jin L, Williamson A, Banerjee S, Philipp I, Rape M. Mechanism of ubiquitin-chain formation by the human anaphase-promoting complex. *Cell*. 2008; 133:653–65. [PubMed: 18485873]



37. Summers MK, Pan B, Mukhyala K, Jackson PK. The unique N terminus of the UbcH10 E2 enzyme controls the threshold for APC activation and enhances checkpoint regulation of the APC. *Mol Cell*. 2008; 31:544–56. [PubMed: 18722180]
38. Wickliffe KE, Lorenz S, Wemmer DE, Kuriyan J, Rape M. The mechanism of linkage-specific ubiquitin chain elongation by a single-subunit E2. *Cell*. 2011; 144:769–81. [PubMed: 21376237]
39. Xu P, Duong DM, Seyfried NT, Cheng D, Xie Y, Robert J, et al. Quantitative proteomics reveals the function of unconventional ubiquitin chains in proteasomal degradation. *Cell*. 2009; 137:133–45. [PubMed: 19345192]
40. Goto E, Yamanaka Y, Ishikawa A, Aoki-Kawasumi M, Mito-Yoshida M, Ohmura-Hoshino M, et al. Contribution of lysine 11-linked ubiquitination to MIR2-mediated major histocompatibility complex class I internalization. *J Biol Chem*. 2010; 285:35311–9. [PubMed: 20833710]
41. Dynek JN, Goncharov T, Dueber EC, Fedorova AV, Izrael-Tomasevic A, Phu L, et al. c-IAP1 and UbcH5 promote K11-linked polyubiquitination of RIP1 in TNF signalling. *EMBO J*. 2010; 29:4198–209. [PubMed: 21113135]
42. Ciechanover A. The ubiquitin-proteasome pathway: on protein death and cell life. *EMBO J*. 1998; 17:7151–60. [PubMed: 9857172]
43. Snoek BC, de Wilt LH, Jansen G, Peters GJ. Role of E3 ubiquitin ligases in lung cancer. *World journal of clinical oncology*. 2013; 4:58–69. [PubMed: 23936758]
44. Christian PA, Fiandalo MV, Schwarze SR. Possible role of death receptor-mediated apoptosis by the E3 ubiquitin ligases Siah2 and POSH. *Molecular cancer*. 2011; 10:57. [PubMed: 21586138]

### Statement of Translational Relevance

Lung cancer, especially NSCLC, is the leading cause of cancer death in the USA and around the world. Although great efforts have been made to develop targeted therapies against NSCLC, the five-year survival of patients remains low. Thus, development of specific biomarkers and validation of attractive targets remain a priority and challenge. In this study, we report that UBE2F is highly expressed in NSCLC tissues, which is negatively associated with overall survival. Furthermore, UBE2F overexpression promotes cancer cell growth both in vitro and in vivo, whereas UBE2F knockdown selectively inhibits growth of lung cancer cells, but not non-transforming bronchial cells. Mechanistically, UBE2F down-regulates NOXA through promoting its ubiquitylation via a novel K11 linkage. Our study validates UBE2F as an attractive lung cancer target and provides an appealing rationale for future discovery of specific UBE2F inhibitors against NSCLC.

Author Manuscript

Author Manuscript

Author Manuscript

Author Manuscript

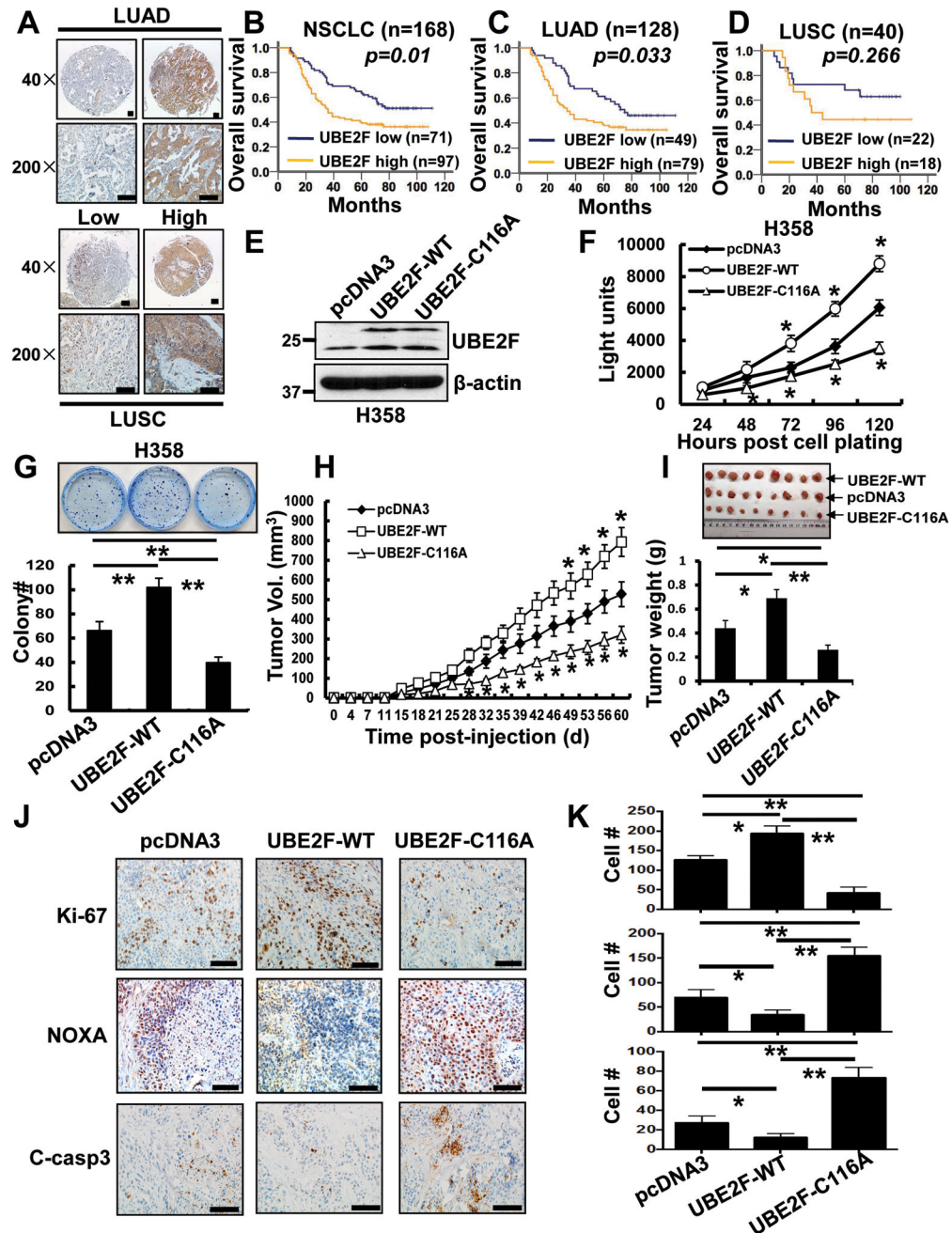


**Figure 1. UBE2F high expression in human lung tumor tissues associates with poor patient survival and UBE2F overexpression promotes the growth of lung cancer cells both *in vitro* and *in vivo***

(A) UBE2F staining in lung tumor tissues: LUAD (lung adenocarcinoma) and LUSC (lung squamous carcinoma) tissue microarrays were stained by using Abs against UBE2F (Abcam). (B-D) Kaplan-Meier curves to show association between the levels of UBE2F expression and overall survival of patients with NSCLC (B), LUAD (C), and LUSC (D). (E) Expression of UBE2F: indicated plasmids were transfected into H358 cells individually, followed by G418 selection for 2 weeks. The stable clones were pooled and subjected to IB.

**(F&G)** Effects of UBE2F on cell growth and survival: H358 stable clones were seeded into 96-well plates, followed by ATPlite assay after incubation for various time points (F); or seeded into 60-mm dishes at 800 cells per dish in duplicate, and incubated at 37°C for 14 days, followed by 0.05% methylene blue staining and colony counting (G). Shown is mean  $\pm$  SD from three independent experiments (\*,  $p < 0.05$ ; \*\*,  $p < 0.01$ ); **(H&I)** Effects of UBE2F on tumor growth in xenograft models:  $5 \times 10^6$  of H358 stable clones were inoculated subcutaneously in both flanks of nude mice, with 5 mice in each group. The tumor growth was monitored up to 60 days and growth curve plotted (H). Tumor tissues were weighed and photographed at 60 days (I). Student's *t* test was used to compare each experimental group with the control group. Shown are mean  $\pm$  SEM, \*,  $p < 0.05$ ; \*\*,  $p < 0.01$ ; **(J&K)** IHC staining of mouse tumor tissues: tumor tissues were fixed, sectioned, and stained. Scale bars: 100  $\mu$ M. Positively stained cells were counted out of a total of 500 cells on average from 3 independent tumors derived from 3 mice per group. Shown are mean  $\pm$  SD, \*,  $p < 0.05$ ; \*\*,  $p < 0.01$ .

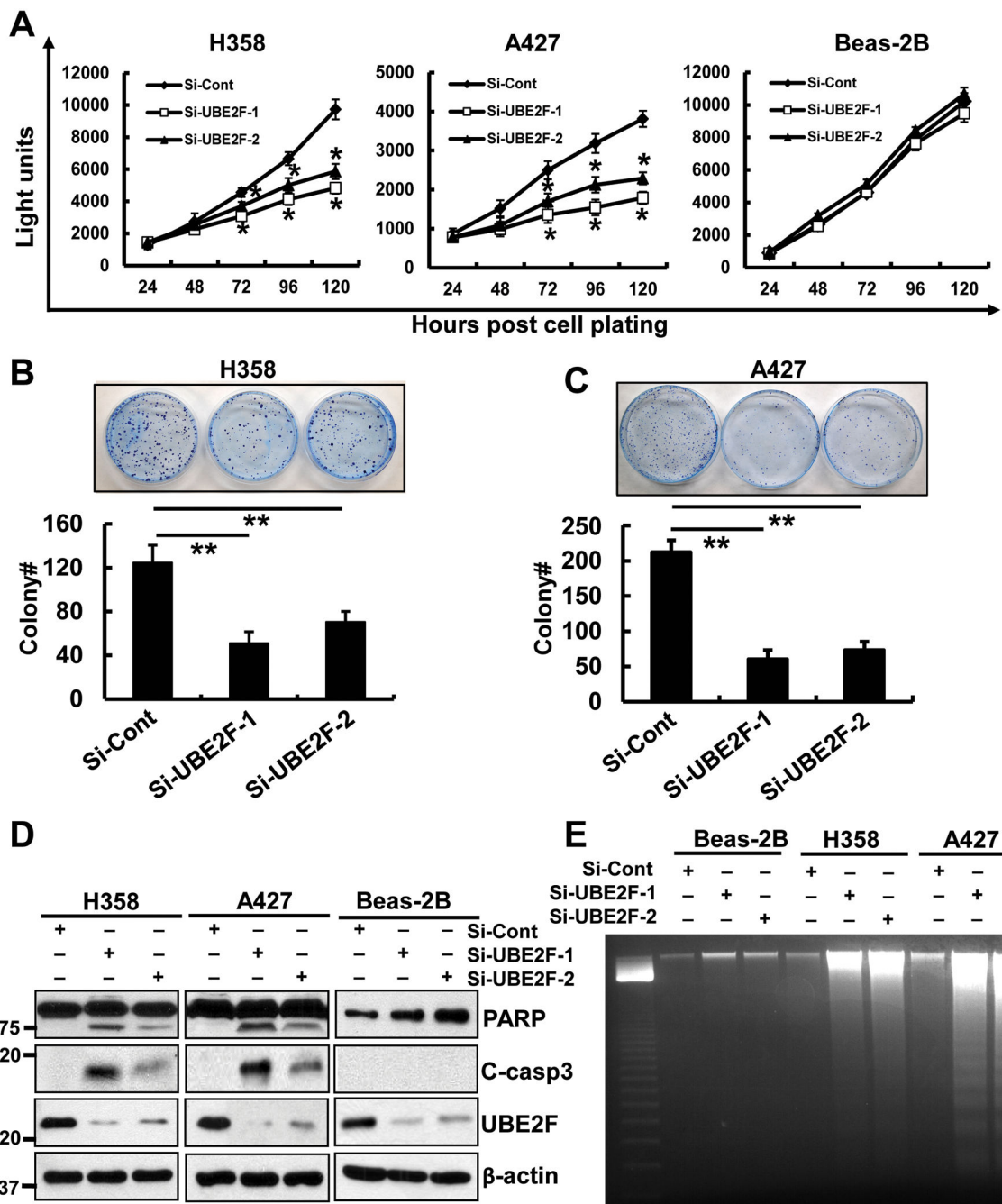


**Figure 2. UBE2F silencing selectively inhibits growth of lung cancer cells by inducing apoptosis** (A) Cell growth assay: after UBE2F siRNA silencing, cells were seeded into 96-well plates at 3,000 per well in triplicate and measured by ATPlite assay over periods up to 120 hrs. Shown is mean  $\pm$  SD from three experiments (\*,  $p < 0.05$ ); (B&C) Clonogenic survival assay. Cells after UBE2F siRNA silencing were seeded into 60-mm dishes at 800 cells (C; H358) or 600 cells (D; A427) per dish in duplicate, and incubated at 37°C for 14 days, followed by 0.05% methylene blue staining and colony counting. Results are representative of three independent experiments (mean  $\pm$  SD; \*\*,  $p < 0.01$ ); (D&E) UBE2F knockdown induces

apoptosis in lung cancer cells: cells were transfected with si-Cont and si-UBE2F for 48 hrs, followed by IB (E) and DNA fragmentation (F). Results are representative of three independent experiments.

Author Manuscript

Author Manuscript

Author Manuscript

Author Manuscript



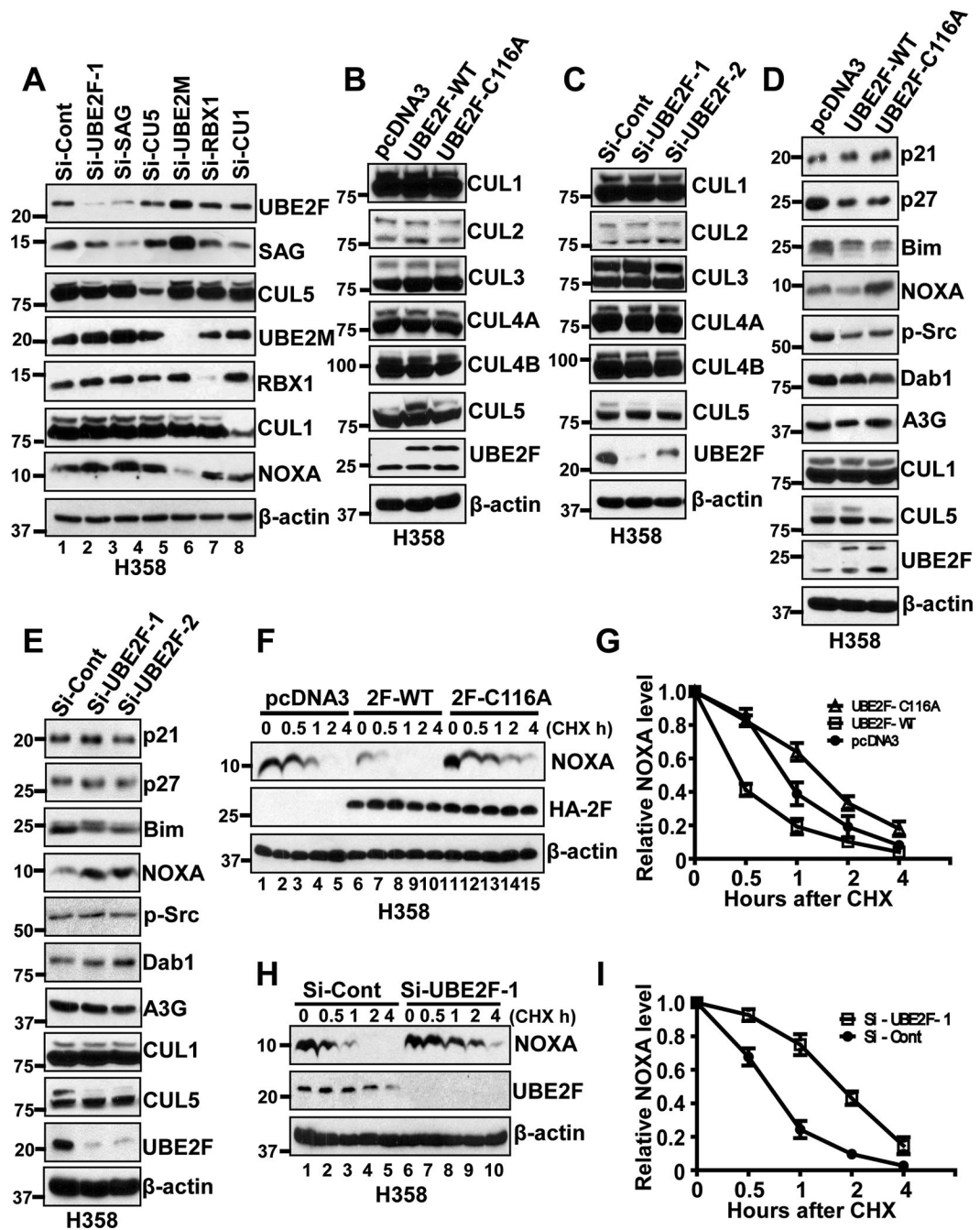


**Figure 3. UBE2F negatively regulates NOXA level in lung cancer cells**

(A) NOXA is increased upon silencing of CUL5 components. H358 cells were transfected with indicated siRNAs for 48 hrs. Cells were then harvested for IB. (B-E) Regulation of Cullins, known CUL5 substrates, and NOXA by UBE2F: H358 stable clones (B&D), expressing wild-type or enzymatic dead UBE2F mutant, along with pcDNA control, were harvested for IB. H358 (C&E) cells were transfected with si-Cont or si-UBE2F-1/-2 and harvested 48 hrs later for IB. (F-I) Measurement of NOXA  $T_{1/2}$ : lung cancer cells were either transfected with indicated plasmids (F&G) or siRNAs (H&I). Cells were then

switched to fresh medium (10% FBS) containing cycloheximide (CHX) and incubated for indicated time periods before being harvested for IB (F&H). The band density was quantified using ImageJ software and plotted (G&I).

Author Manuscript

Author Manuscript

Author Manuscript

Author Manuscript

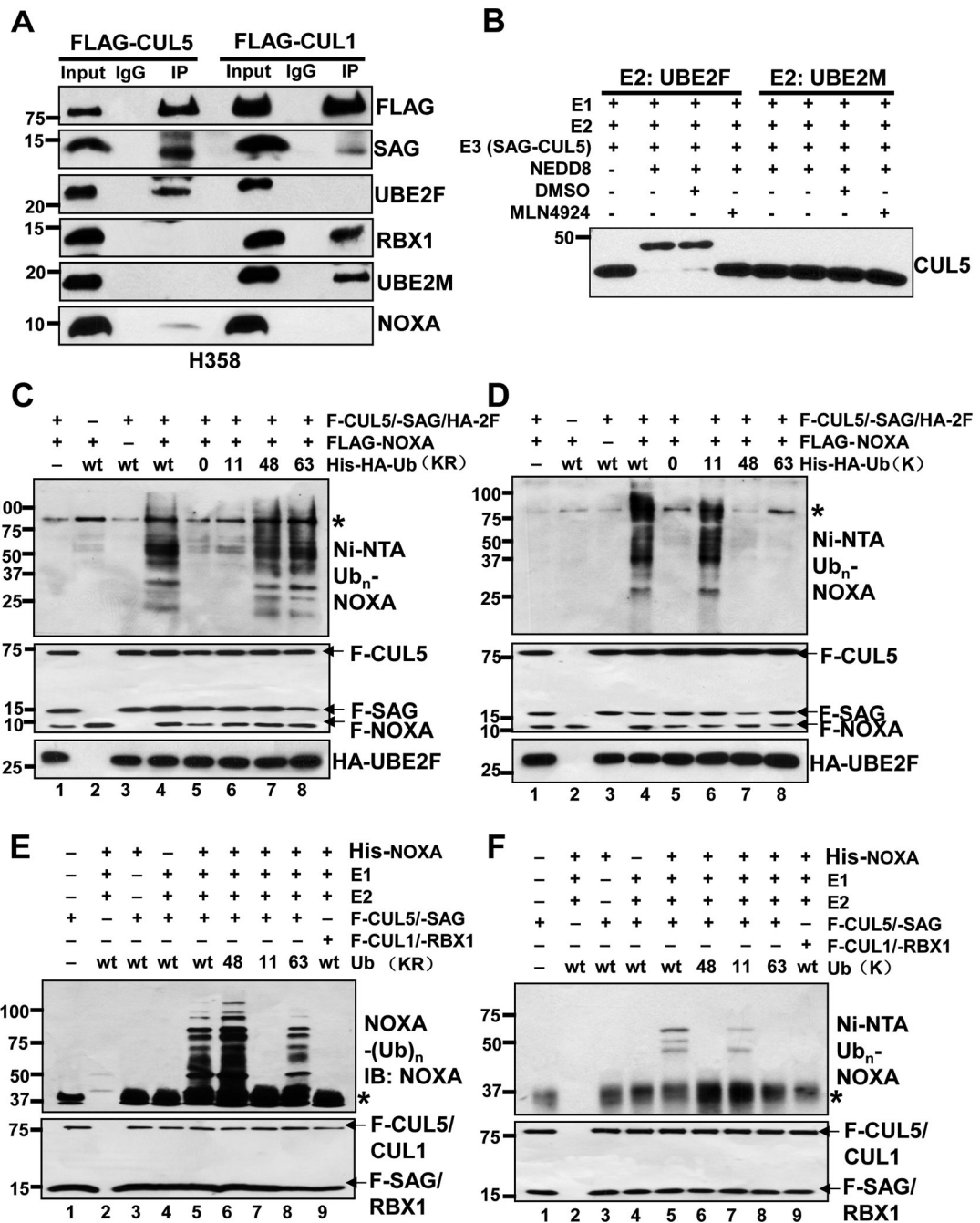


**Figure 4. CRL5 facilitates poly-ubiquitylation of NOXA via the K11-linkage**

(A) UBE2F, CUL5, SAG, and NOXA bind to each other. H358 cells were transfected with FLAG-CUL5 or FLAG-CUL1, and lysates were immunoprecipitated using FLAG-tagged beads or IgG control, followed by IB to detect endogenous proteins as indicated. The 10% of the extracts used for the input. (B) UBE2F/SAG specifically promotes CUL5 neddylation using an *in vitro* neddylation assay. APP-BP1/UBA3, NEDD8, co-purified full-length-SAG/truncated-CUL5 (398–780) proteins, and UBE2F or UBE2M, were incubated in a reaction mixture with or without addition of MLN4924 for 10 min at room temperature, followed by

IB by using CUL5 Ab. **(C&D)** CRL5 promotes poly-ubiquitylation of NOXA via the K11-linked chain using an *in vivo* ubiquitylation assay. 293 cells were co-transfected with pcDNA3, FLAG-NOXA (substrate), E3 complex (FLAG-CUL5; FLAG-SAG; HA-UBE2F), and wild type His-HA-tagged ubiquitin or various ubiquitin mutants, as indicated. Whole cell extracts and Ni-NTA affinity purified fractions were analyzed by IB with anti-NOXA antibody (Mouse; Millipore). \*: non-specific band. **(E&F)** CRL5 promotes poly-ubiquitylation of NOXA via K11-linked chain, using an *in vitro* ubiquitylation assay. The 293 cells were co-transfected with FLAG-CUL5 and FLAG-SAG (F-CUL5/-SAG), or FLAG-CUL1 and -RBX1 (F-CUL1/-RBX1). Cells were then collected 48 hrs post transfection and lysed, followed by pull-down with FLAG-tagged beads. FLAG-tagged CUL5/SAG or CUL1/RBX1, which serve as the E3 complex, were then incubated in a reaction mixture containing ATP, ubiquitin, E1, E2 (UBE2S and UBCH10), and substrate (purified NOXA protein), followed by ubiquitylation assay. \*: non-specific band.

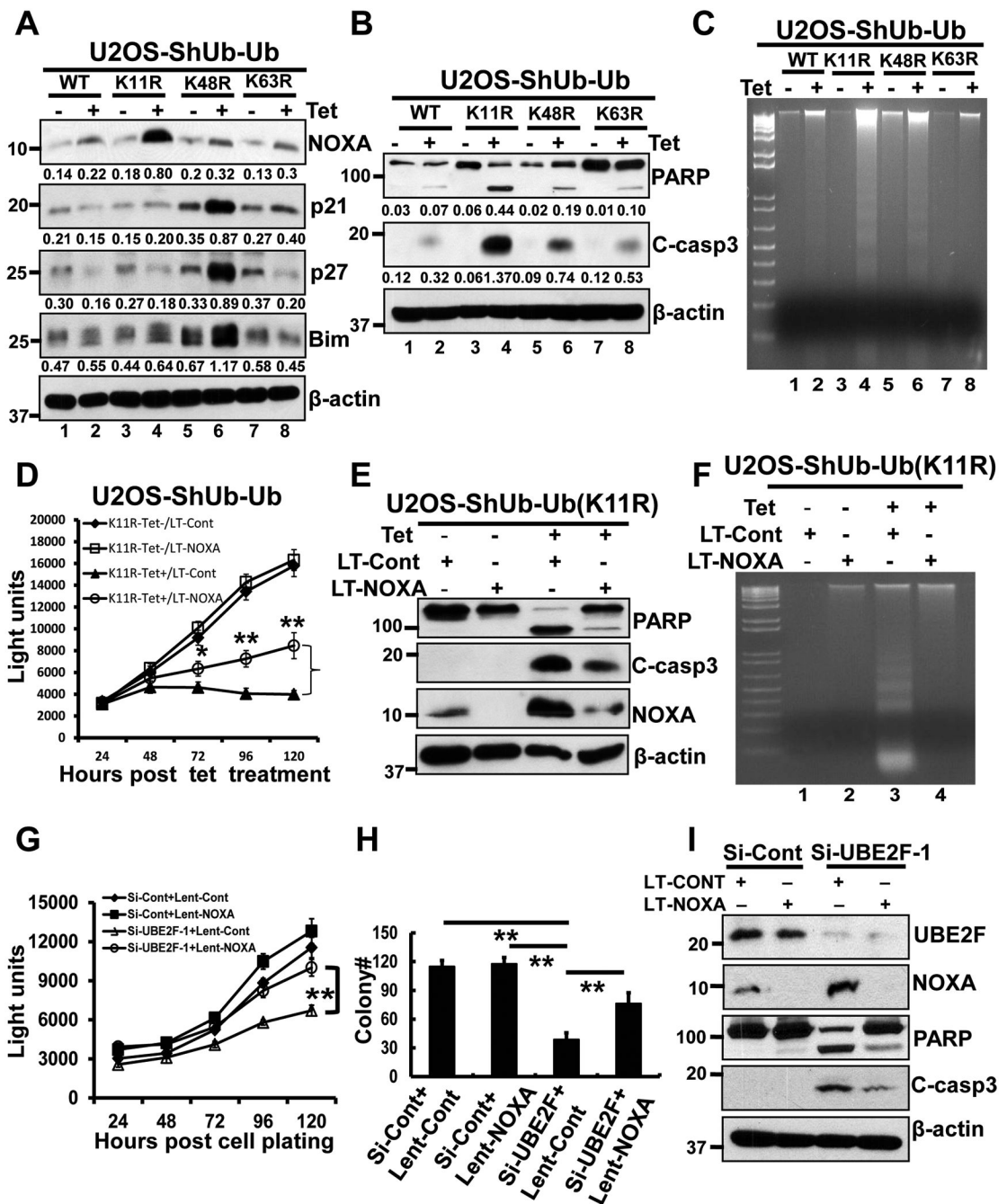


**Figure 5. NOXA is selectively accumulated and responsible for the apoptotic phenotype in tetracycline-induced U2OS-shUb-Ub (K11R) cells**

(A) NOXA is specifically accumulated in the cells with tetracycline-induced replacement of endogenous Ub with Ub (K11R): U2OS-shUb-Ub (WT), -Ub (K11R), -Ub (K48R), and -Ub (K63R) cells were treated with or without tetracycline (1 mg/mL) for 4 days before cell lysates were prepared for IB. The ratio of the intensity of the bands corresponded to NOXA, p21, p27, Bim and β-actin, were shown in the bottom. Results are representative of three different experiments. (B&C) Enhanced apoptosis was detected in the U2OS-shUb-Ub

(K11R) cells upon tetracycline treatments. Cells were seeded in duplicate and treated with or without tetracycline (1 mg/mL) for 4 days and then collected for IB (B) and DNA fragmentation assay (C). Results are representative of three different experiments. **(D-F)** NOXA knockdown reverses the growth suppression and apoptotic induction in U2OS-shUb-Ub (K11R) cells. U2OS-shUb-Ub (K11R) cells were seeded in duplicate and treated with or without tetracycline (1 mg/mL) for 3 days, and then transfected with LT-Cont and LT-NOXA, followed by ATPlite assay 72 hrs later (D), IB (E) and DNA fragmentation assay (F). **(G-I)** NOXA knockdown rescues apoptotic phenotypes induced by UBE2F silencing. H358 cells were transfected with si-Cont and si-UBE2F first, and then with LT-Cont and LT-NOXA, and incubated for 72 hrs. Cells were split and seeded for ATPlite assay (G), clonogenic assay (H), and IB (I). Shown are mean  $\pm$  SD; \*\*,  $p < 0.01$ . Results are all representative of three different experiments.



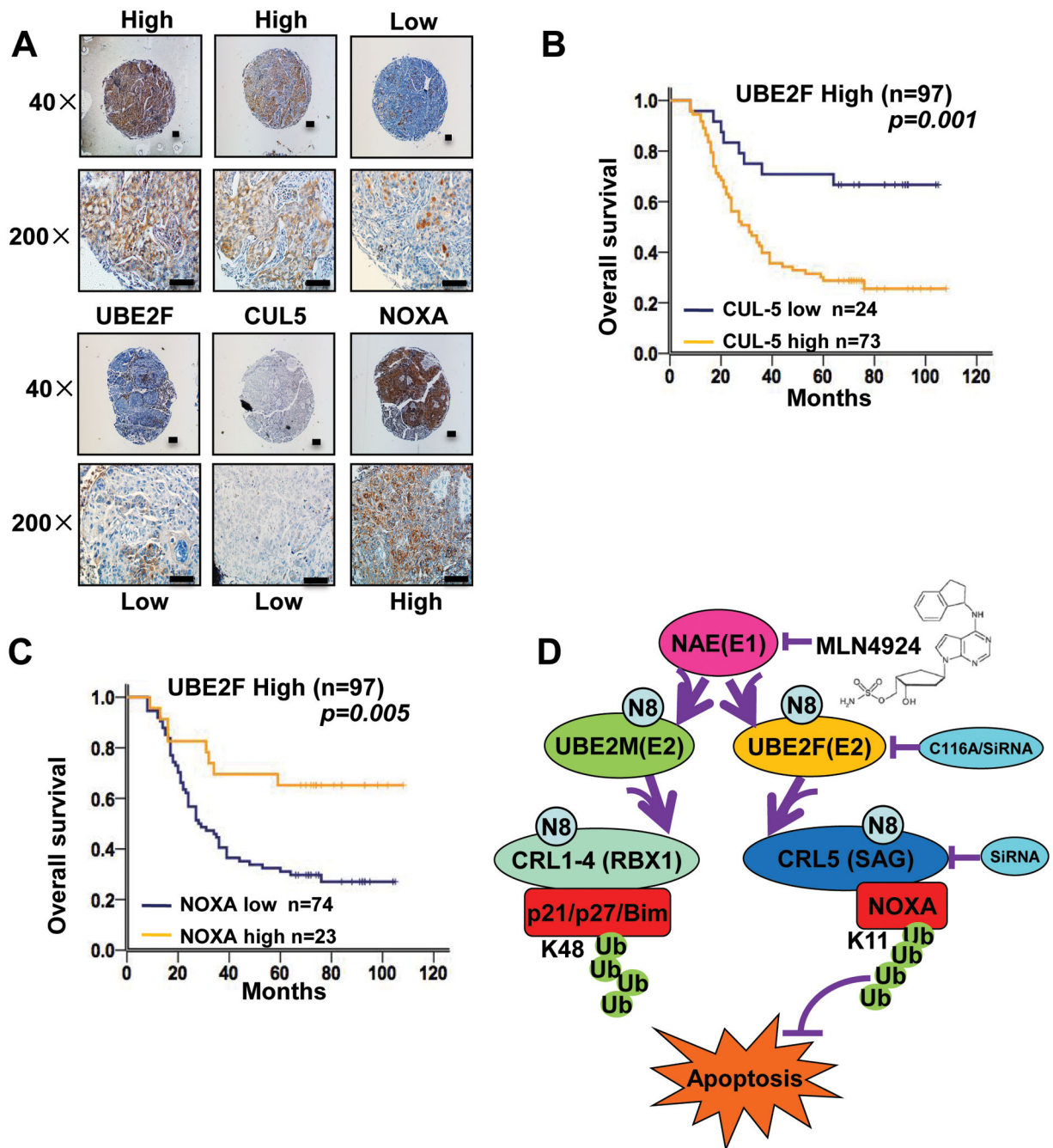


**Figure 6. Expression of UBE2F, CUL5, and NOXA in lung cancer tissues and their association with patient survival**

(A) UBE2F, CUL5, and NOXA staining in lung tumor tissues: LUAD (lung adenocarcinoma) and LUSC (lung squamous carcinoma) tissue microarrays were stained by using Abs against UBE2F (Abcam), CUL5 (Sata cruz) and NOXA (Millipore). (B&C) Kaplan-Meier estimation of overall survival between the levels of CUL5 (E), NOXA (F) and overall survival of patients with high UBE2F expression. (D) A working model. UBE2M-RBX1 neddylates CUL1-4 to activate CRL1-4 for substrate ubiquitylation via the K48-

linkage, followed by degradation, while UBE2F-SAG neddylates CUL5 to activate CRL5 for NOXA ubiquitylation via the K11-linkage and subsequent degradation, leading to cell survival. Thus, targeting CRL5 would cause NOXA accumulation to induce apoptosis and inhibit tumorigenesis.

Author Manuscript

Author Manuscript

Author Manuscript

Author Manuscript